REGULAR ARTICLE

SCANDINAVIAN JOURNAL OF
Immunology AN INTERNATIONAL MONTHLY JOURNAL WILEY

Exploring the role of the multiple sclerosis susceptibility gene *CLEC16A* in T cells

Anna M. Eriksson[1,2] | Ingvild Sørum Leikfoss[1,2,3] | Greger Abrahamsen[4] |
Vibeke Sundvold[4] | Martine Mesel Isom[1] | Pankaj K. Keshari[1,2] | Torbjørn Rognes[5,6] |
Ole J. B. Landsverk[7] | Steffan D. Bos[1,2] | Hanne F. Harbo[1,2] | Anne Spurkland[4] |
Tone Berge[3,8]

[1]Department of Neurology, Oslo University Hospital, Oslo, Norway

[2]Institute of Clinical Medicine, University of Oslo, Oslo, Norway

[3]Neuroscience Research Unit, Department of Research, Innovation and Education, Oslo University Hospital, Oslo, Norway

[4]Department of Molecular Medicine, Institute of Basic Medical Sciences, University of Oslo, Oslo, Norway

[5]Department of Informatics, University of Oslo, Oslo, Norway

[6]Department of Microbiology, Oslo University Hospital, Oslo, Norway

[7]Department of Pathology, Oslo University Hospital, Oslo, Norway

[8]Department of Mechanical, Electronic and Chemical Engineering, Oslo Metropolitan University, Oslo, Norway

Correspondence
Tone Berge, Department of Mechanical, Electronic and Chemical Engineering, Oslo Metropolitan University, Postboks 4, St. Olavs plass, Oslo 0130, Norway.
Email: tone.berge@oslomet.no

Abstract

C-type lectin-like domain family 16 member A (*CLEC16A*) is associated with auto-immune disorders, including multiple sclerosis (MS), but its functional relevance is not completely understood. *CLEC16A* is expressed in several immune cells, where it affects autophagic processes and receptor expression. Recently, we reported that the risk genotype of an MS-associated single nucleotide polymorphism in *CLEC16A* intron 19 is associated with higher expression of *CLEC16A* in CD4$^+$ T cells. Here, we show that *CLEC16A* expression is induced in CD4$^+$ T cells upon T cell activation. By the use of imaging flow cytometry and confocal microscopy, we demonstrate that CLEC16A is located in Rab4a-positive recycling endosomes in Jurkat TAg T cells. *CLEC16A* knock-down in Jurkat cells resulted in lower cell surface expression of the T cell receptor, however, this did not have a major impact on T cell activation response in vitro in Jurkat nor in human, primary CD4$^+$ T cells.

1 | INTRODUCTION

A single nucleotide polymorphism (SNP) in the *C-type lectin-like domain family 16 member A* (*CLEC16A*) gene was among the first genetic variants outside the human leucocyte antigen (HLA) region that showed evidence of association in the first genome-wide association study (GWAS) performed in multiple sclerosis (MS).[1] *CLEC16A* has since then been established as an MS-susceptibility gene.[2-11] SNPs in *CLEC16A* are also associated with several other autoimmune diseases, including type 1 diabetes,[5,12-16] Crohn's disease,[17] Addison's disease[18] and rheumatoid arthritis.[19,20] These studies support a general role for CLEC16A in development of autoimmunity. How CLEC16A contributes to autoimmunity and inflammation is however poorly understood.

Ema, the CLEC16A orthologue in *Drosophila melanogaster*, has been shown to regulate endosomal trafficking and maturation as well as autophagy.[21,22] Also, in mouse and humans, CLEC16A plays a role in autophagic processes as observed in thymic epithelial cells,[23] Purkinje cells,[24] pancreatic β-cells,[25,26] adipose tissue[27] and in the kidney epithelial cell line HEK293T.[28] Furthermore, in splenic B and T cells from *CLEC16A* knockout mice, mitophagy is disrupted.[29] In human antigen-presenting cells, CLEC16A regulates HLA-II expression via late endosomal biogenesis,[30] and in murine natural killer (NK) cells, CLEC16A modulates receptor expression.[31]

Even though functional and epigenetic annotation studies suggest that multiple components of the immune system are involved in MS; T cells, and in particular CD4^{+} T cells, are considered major players in MS pathogenesis.[10,32,33] We recently showed that the MS-risk allele of an MS-associated SNP in intron 19 of *CLEC16A* correlates with higher expression levels of *CLEC16A* in human CD4^{+} T cells.[34] In the current study, we analysed the function of CLEC16A in T cells using the Jurkat TAg T cell line and primary human CD4^{+} T cells. We show that CLEC16A localizes to Rab4a-positive recycling endosomes in Jurkat cells and its expression is induced upon activation of CD4^{+} T cells. Knocking down its expression did not influence starvation-induced autophagy and had only a marginal impact on T cell activation. Our data indicate a T cell-specific localization of CLEC16A to Rab4a-positive endosomes; however, its role in T cells is still enigmatic.

2 | MATERIALS AND METHODS

2.1 | Antibodies and reagents

Primary antibodies used were as follows: anti-LAMP1 (Abcam), anti-TGN46 (Bio-Rad), anti-LC3B (Cell Signaling Technologies), anti-CLEC16A (Thermo Fisher Scientific and Merck), anti-GAPDH and anti p62/SQSTM1 (D-3) (Santa Cruz Biotechnology), anti-actin (Sigma-Aldrich), allophycocyanin (APC)-conjugated anti-CD69 (Immunotools), APC-conjugated TCR alpha/beta (IP26, Molecular Probes, Thermo Fisher Scientific), APC-conjugated anti-human CD25 (MEM-181. Immunotools), phycoerythrin (PE)-conjugated anti-human HLA-DR (L203, R&D Systems) and anti-CD3ε (clone OKT3, American Type Culture Collection (ATCC)). Secondary antibodies used were as follows: Alexa Fluor (AF) 647-conjugated anti-rabbit IgG, AF647-conjugated anti-mouse IgG and AF555-conjugated anti-mouse IgG2a (Life Technologies, Thermo Fisher Scientific), horseradish peroxidase (HRP)-conjugated goat anti-mouse IgG, goat anti-rabbit IgG and mouse anti-goat IgG (Jackson Immuno Research Laboratories Europe Ltd.). Isotype controls used were APC-conjugated anti-IgG1 (Immunotools). Dynabeads® Human T-Activator CD3/CD28 for T Cell Expansion and Activation and LIVE/DEAD Fixable Near-IR Dead Cell Stain Kit were from Thermo Fisher Scientific.

C-type lectin-like domain family 16 member A -specific siRNA (ON-TARGET plus SMARTpool siRNA) and control siRNA (ON-TARGET plus Non-targeting Pool) were obtained from Thermo Fisher Scientific and Hoechst from Life Technologies. Phorbol 12-myristate 13-acetate (PMA), paraformaldehyde (PFA), saponin, sodium azide, ionomycin calcium salt from *Streptomyces* and dimethyl sulphoxide (DMSO) were obtained from Sigma-Aldrich. Bovine serum albumin (BSA) was obtained from Bio-Rad and Bafilomycin A1 (BafA1) from Bio Vision.

2.2 | Plasmids

pCMV6-CLEC16A-myc-DDK was obtained from Origene Technologies (TrueORF™ Precision Shuttle Vector system), pEGFP-N3 from Clontech Laboratories (Takara Bio), pcDNA3-Rab4a (cloneID: RAB04A000) in from UMR cDNA Resource Center and pmax-GFP from Lonza. pMep4-Rab5-mCherry has been described previously.[35] Rab4a was subcloned into *Eco*RI-*Xho*I sites of pEGFP-C2 (Clontech Laboratories). EGFP was replaced with mCherry using Gibson assembly multiplex PCR. C-terminally and N-terminally GFP-tagged CLEC16A was generated by subcloning a blunted *Eco*RI/*Not*I digest of pCMV6-CLEC16A-myc-DDK into the *Sma*I site of pEGFP-N3 (Clontech Laboratories; C-term tag) and *Sma*I and blunted *Xba*I sites of pEGFP-C1 (Clontech Laboratories; N-term tag). The pCMV6-empty vector was generated by removing CLEC16A from pCMV6-CLEC16A-myc-DDK by digestion with *Bam*HI and *Pme*I, blunting and re-ligation. The subcloned constructs were confirmed by DNA sequencing (GATC Biotech AG).

2.3 | RNA isolation, synthesis of cDNA and quantitative real-time PCR

RNA was isolated using the RNeasy Plus Mini Kit and QiaShredder spin column (both from Qiagen, Hilden) according to the manufacturer's protocol. RNA concentration, quality and integrity were measured using the NanoDrop 2000 c Spectrophotometer (Thermo Fisher Scientific Inc) and Agilent 2100 Bioanalyzer (Agilent Technologies), respectively. RNA with RNA integrity number values above 6.0 was included.

Reverse transcription was performed as previously described[34]; 100 ng RNA in 10 μL reaction and a standard curve with 1:2 fold dilution series (500-7.8 ng). The quantitative real-time PCR (RT-qPCR) was performed as previously described[34] using *18S rRNA* (Hs99999901_s1), *TATA-box binding protein* (*TBP*; Hs99999910_m1), *RNase P* (4316844) and *CLEC16A* (HS00389799_m1; all from Applied Biosystems).

2.4 | Cell culture

$CD14^{high}CD16^-$ monocytes, $CD56^+$ NK and $CD19^+$ B cells were isolated from buffy coat as described.[36-38] $CD4^+$ and $CD8^+$ T cells were isolated from blood of healthy donors as described elsewhere.[39]

$CD4^+$ T cells were maintained in X-VIVO 15 chemically defined, serum-free haematopoietic cell medium (Lonza) at 37°C with 5% CO_2. Jurkat TAg T cells[40] ($0.3\text{-}1.5 \times 10^6$ cells/mL) were maintained at 37°C and 5% CO_2 in RPMI 1640 with L-glutamine and 10% fetal calf serum (FCS), 1 mmol/L sodium pyruvate, 1 mmol/L non-essential amino acids, penicillin (100 U/mL), streptomycin (100 U/mL) (all from GIBCO-BRL, Life Technologies) and 0.05 mmol/L β-mercaptoethanol (Sigma-Aldrich).

2.5 | Transfection and activation

Jurkat TAg T cells (15×10^6 cells) were transfected with 1 μmol/L siRNA or 1-5 μg plasmid DNA. Cells were pulsed using BTX electroporator (Genetronix) at 240 V/25 ms Transfected cells were supplied with RPMI 1640 with L-glutamine with 5% FCS, 1 mmol/L sodium pyruvate, 1 mmol/L non-essential amino acids and 0.05 mmol/L β-mercaptoethanol at 37°C with 5% CO_2. Forty-eight hours later, Jurkat T cells were either left unstimulated (DMSO) or stimulated for 24 hours with PMA and ionomycin or left unstimulated (PBS) or stimulated for 4, 24 and 48 hours with 2 μg/mL plate-bound OKT3.

$CD4^+$ T cells were transfected with 0.5 μmol/L siRNA or 2.5 μg pmax-GFP plasmid using AMAXA Nucleofector I with U-14 program (Amaxa Biosystems) according to the kit procedure (Human T cell Nucleofector Kit for unstimulated

human T cells, Lonza). After transfection, cells were incubated with preheated LGM-3 medium (Lonza) supplemented with 10% FCS at 37°C, 5% CO_2. Twenty hours later, the $CD4^+$ T cells were activated with anti-CD3/CD28-coated beads (one bead per cell) in X-VIVO 15.

2.6 | Flow cytometry

Cells were blocked in PBS with 5% FCS (for staining of Jurkat cells) or human serum (for staining of $CD4^+$ T cells) (H4522; Sigma-Aldrich) and 0.05% sodium azide prior to staining with indicated antibodies diluted in PBS with 1% FCS and 0.05% sodium azide for 30 minutes on ice. Flow cytometry was performed using Attune Acoustic Focusing Cytometer (Thermo Fisher Scientific) or FACSCanto II flow cytometer with FACSDiva (BD Biosciences). Data were analysed by FCS Express 6 (De Novo Software). Pre-gating for single, living cells was performed.

2.7 | Cell starvation and autophagy

After transfection (48 hours), cells were incubated in Earle's Balanced Salt Solution (EBSS; GIBCO-BRL) with or without 100 nmol/L BafA1, or in RPMI 1640 supplied with 5% FCS, 1 mmol/L sodium pyruvate and 1 mmol/L non-essential amino acids with or without BafA1, for 4 hours.

2.8 | Confocal microscopy

Cells were stained with 1 μg/mL Hoechst (Life Technologies) and applied on poly-L-lysine-coated cover slides (VWR international). Cells were fixed in 3% PFA and mounted in a SlowFade® Gold antifade reagent (Invitrogen, Thermo Fisher Scientific). Cells were stained with anti-LAMP1 or anti-TGN46 primary antibody and AF647 anti-rabbit IgG secondary antibody diluted in PBS with 0.25% BSA and 0.05% saponin. To analyse internalized TCRs, cells were incubated with OKT3 on ice for 30 minutes, then at 37°C and 5% CO_2 for 40 minutes, before staining.

Confocal microscope (Olympus Fluoview 1000/BX61WI) with 405, 488, 543 and 633 nm lasers and UPlanSApo 60x/ 1.35 NA oil (Olympus) objective was used. Image processing was performed in Fiji (http://fiji.sc/wiki/index.php/Downloads), Photoshop and Illustrator CS6 (both from Adobe Systems Inc).

2.9 | Imaging flow cytometry

Cells were stained with 1 μg/mL of Hoechst, fixed with 2% PFA and resuspended in PBS containing 1% FCS and 0.05%

sodium azide. 5×10^4 cells were acquired on a 12-channel Image stream^X Mark I/II imaging flow cytometer (IFC) with a 40× objective (Amnis), as described.[41] Co-localization was analysed using IDEAS 6.1v software (Amnis). A compensation matrix generated from single-stained cells using raw image files was applied to compensate for spectral overlap. Co-localization was analysed by applying the Bright Detail Similarity feature in IDEAS.[42] To establish gates for close proximity, a negative control was generated by expressing Rab5-mCherry in Hoechst-stained Jurkat T cells, and a positive control by expressing both Rab4a-mCherry and Rab4a-GFP in Jurkat T cells.

2.10 | Recycling assay

Forty-eight hours after transfection, cells were surface labelled with anti-CD3 (clone OKT3) on ice for 30 minutes and resuspended in RPMI 1640 with 1% BSA to allow OKT3 internalization for 40 minutes (37°C and 5% CO_2). Cells were washed before drop-wise addition of stripping solution (PBS with 2% BSA and 0.1% sodium azide, pH 2.5). Samples were incubated for 30 seconds prior to addition of RPMI 1640 with 1% BSA and incubated for 0, 10, 20 and 40 minutes (37°C and 5% CO_2), allowing re-emerging of internalized OKT3. At each stage, cell surface OKT3 was stained with AF555 anti-mouse IgG2a on ice for 30 minutes prior to analysis of duplicate samples by flow cytometry. Percentage of internalized receptor was calculated by the equation: $\left(T_0 - T_i/T_0\right) \times 100$. Percentage recycled TCR receptor was calculated by the equation: $\left(T_t - T_s\right) / \left(T_0 - T_i\right) \times 100$. T_0–median fluorescence intensity (MFI) of the sample after OKT3 surface labelling, T_i–MFI after internalization of receptor, T_s–MFI after antibody stripping and T_t–MFI after time 't'.

2.11 | Western blotting

Cells were lysed in RIPA buffer (Thermo Scientific), separated by SDS polyacrylamide gel electrophoresis (Criterion gels, Bio-Rad) and blotted onto polyvinylidene fluoride membrane (Trans-blot turbo transfer system with its transfer pack, Bio-Rad). Membranes were blocked in 5% skimmed milk (Sigma) in Tris-buffered saline (TBS, pH 7.4) containing 0.1% Tween 20 (TBS-T; Medicago) following incubation with antibodies in TBS-T with 5% skimmed milk. Bound antibodies were visualized by incubation with secondary HRP-conjugated antibodies and Super Signal West Pico stable peroxide solution (Pierce Biotechnology). Densitometry of the Western blots was performed in Image Studio Lite version 5.2.5 (Li-Cor). The quantities of LC3II and p62 were determined relative to a housekeeping protein (GAPDH or Actin) .

2.12 | Statistical analyses

As specified in the corresponding figure legends, two-sided Student's pair-wise t tests or one sample t tests were performed, for comparison of more than two groups, one-way ANOVA was performed (GraphPad prism 6, Inc). P-values below .05 were considered significant.

3 | RESULTS

3.1 | CLEC16A mRNA expression is induced upon CD4$^+$ T cell activation

The highest expression of *CLEC16A* is found in testis and in the Burkitt lymphoma cell line Raji. In addition, *CLEC16A* is also expressed in other immune cells as well as in certain brain cells.[43,44] Here, we assessed *CLEC16A* expression in different primary human immune cell subtypes by quantitative real-time polymerase chain reaction (RT-qPCR) and found that CD4$^+$ and CD8$^+$ T cells as well as CD56$^+$ NK cells express less *CLEC16A* compared to CD19$^+$ B cells and CD14^{high}CD16$^-$ monocytes, with the latter showing highest *CLEC16A* expression (Figure 1A). Moreover, *CLEC16A* expression was induced in CD4$^+$ T cells upon T cell activation using anti-CD3/CD28-coated beads (Figure 1B; 4 hours; $P = .043$, 20 hours; $P = .007$, 41.5 hours; $P = .016$), indicating that CLEC16A might play a role in activated T cells.

3.2 | Cell-specific co-localization of CLEC16A with Rab4a-positive recycling endosomes in Jurkat T cells

Previous studies of CLEC16A and its *Drosophila* orthologue Ema showed that CLEC16A and Ema localize to different subcellular structures in the endosomal system, depending on the cellular model under study, including late endosomes,[30] lysosomes,[25] the endoplasmic reticulum[45] and the Golgi apparatus.[28] In order to analyse whether CLEC16A localizes in the endosomal system also in T cells, Jurkat T cells expressing GFP-tagged CLEC16A were co-transfected with a plasmid expressing mCherry-tagged Rab4a (marker for recycling endosomes) or Rab5 (marker for early endosomes), or labelled with antibodies recognizing the trans-Golgi marker TGN46 or the late endosomal/lysosomal marker LAMP1. Imaging flow cytometry (IFC) with the Bright Detail Similarity feature of the IDEAS software was used to assess how well two fluorescence signals correlate pixel by pixel.[42] We found that about 60% of the cells showed close proximity of CLEC16A and Rab4a and of CLEC16A and Rab5 relative to the positive control (Figure 2A, B). CLEC16A and LAMPI or TGN46 were not in proximity to each other (Figure S1A and Figure 2B).
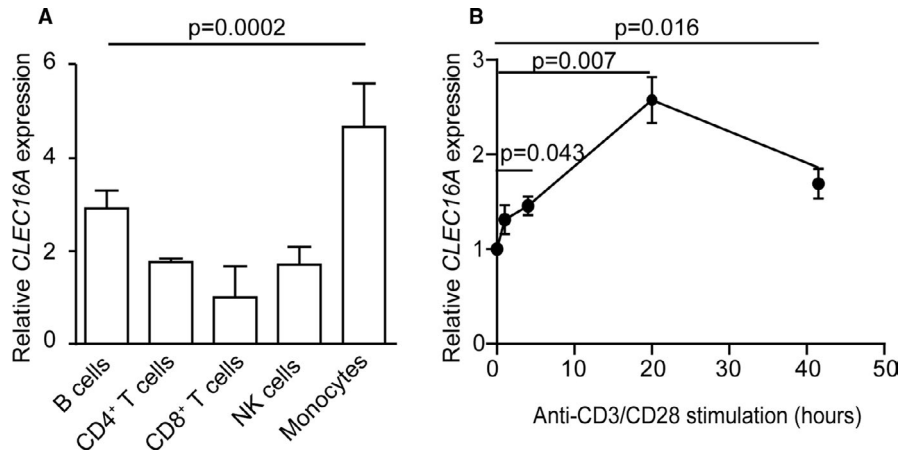
FIGURE 1 *CLEC16A* mRNA expression is induced upon CD4^{+} T cell activation. A, *CLEC16A* expression relative to *RNaseP* in indicated primary immune cells, that is CD19^{+} B cells, CD4^{+} and CD8^{+} T cells, CD56^{+} NK cells and CD14^{high}CD16^{-} monocytes. The relative expression measurements were performed in triplets from three different donors. Median values with standard error of the mean (SEM) are shown ($P = .0002$, one-way ANOVA). B, *CLEC16A* expression relative to *RNaseP* in CD4^{+} T cells activated with anti-CD3/CD28-coated beads for indicated time points. The relative expression measurements were performed in doublets from four different donors. The data display the mean fold change with SEM. Data are analysed by one sample *t* test comparing stimulated samples with unstimulated samples (set to 1). *P*-values <.05 are considered significant

Next, we used confocal microscopy to achieve high-resolution images to confirm and refine the IFC analyses. Confocal microscopy analyses revealed that N-terminally tagged CLEC16A co-localizes with Rab4a-positive recycling endosomes in Jurkat T cells, while no co-localization was observed between CLEC16A and Rab5, TGN46 or LAMP1 (Figure 2C). Confocal analyses of cells expressing CLEC16A with a C-terminal GFP tag, verified co-localization between CLEC16A and Rab4a, showed partly co-localization with low-intensity Rab5 spots and no co-localization with TGN or LAMP1 (Figure S1B).

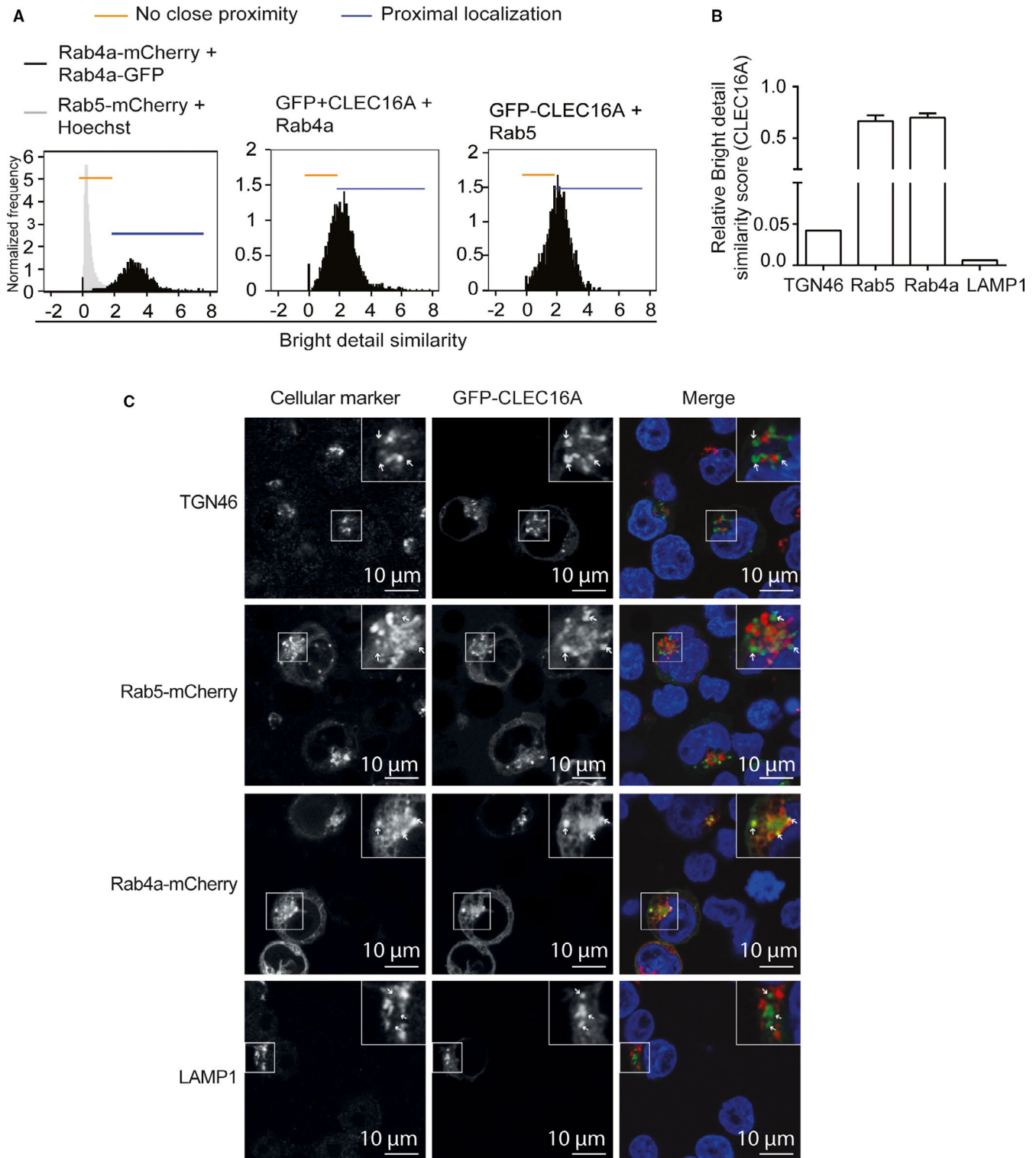## 3.3 | CLEC16A overexpression affects starvation-induced T cell autophagy in Jurkat T cells

Rab4a-positive recycling endosomes act as a source of membranes during autophagosome formation in the initial phase of autophagy.[46,47] Given the importance of CLEC16A for autophagy in both murine and human cells,[23,24,28,31] we thus investigated whether CLEC16A influenced autophagy in human T cells, by either overexpressing or knocking it down in Jurkat T cells. The LC3 and p62 proteins are markers used to monitor autophagy. Induction of autophagy results in conjugation of cytosolic LC3-I to phosphatidylethanolamine in the autophagic membrane, giving rise to lipidated LC3-II.[48] The p62 protein is degraded by autophagy and accumulates upon autophagy inhibition.[49] Autophagy was induced by starvation of transfected Jurkat T cells, in the presence or absence of the lysosomal proton pump inhibitor, BafA1. The autophagic flux was monitored by immunoblotting of endogenous LC3-II (Figure 3).

Overexpression of *CLEC16A* in Jurkat cells resulted in an overall accumulation of LC3-II in cells with the inhibitor present, both with and without starvation (Figure 3A, B; $P = .044$ and $P = .039$). The difference in the p62 levels between BafA1 and vehicle-treated cells represents the amount of p62 that has been recruited into autophagosomes during the treatment period. BafA1-treated cells displayed higher level of p62 compared to control cells. In cells overexpressing *CLEC16A,* there seems to be a slight rise in p62 levels upon BafA1 treatment (Figure 3B right graph), however, this did not reach statistical significance. Knocking down *CLEC16A* expression did not corroborate the LC3II findings, as *CLEC16A* deficiency did not have any effect on LC3-II formation nor p62 levels (Figure 3C, D).

3.4 | Lower TCR cell surface expression in CLEC16A-deficient Jurkat cells

Intracellular TCR has been shown to localize in the Rab4 recycling endosomes.[50,51] Since we were not able to detect any changes in autophagy when knocking down *CLEC16A* expression in T cells, we next tested whether CLEC16A could have an impact on TCR recycling.

To monitor TCR localization in Jurkat T cells following internalization, we surface labelled GFP-CLEC16A expressing Jurkat cells with TCR antibodies (clone OKT3) prior to incubation at 37°C to allow internalization of the antibodies together with the receptors. In these cells, the internalized TCRs co-localized with GFP-tagged CLEC16A (Figure 4A). To determine if CLEC16A is directly involved in TCR recycling, a recycling assay adapted from Patrussi and Baldari[52] was performed (Figure 4B). Jurkat T cells

A

— No close proximity   — Proximal localization

—— Rab4a-mCherry + Rab4a-GFP
—— Rab5-mCherry + Hoechst

GFP+CLEC16A + Rab4a

GFP-CLEC16A + Rab5

B

C

	Cellular marker	GFP-CLEC16A	Merge
TGN46			
Rab5-mCherry			
Rab4a-mCherry			
LAMP1			

were surface stained for TCR antibodies, followed by incubation at 37°C (as above) prior to removal of surface antibodies. The cells were subsequently incubated for indicated time points at 37°C to allow re-emergence of internalized antibodies. At each step, cell surface levels of TCR were measured by flow cytometry (assay schematically depicted in Figure 4B). As expected, we observed a decrease in the fluorescently labelled TCR on the cell surface after internalization, with an additional decrease after acid stripping. After incubating the cells for 10 minutes, the receptors started to re-emerge on the cell surface, as indicated by an increase in TCR cell surface expression (Figure S2A, B).

Prior to internalization, we analysed the cell surface expression of TCR by flow cytometry. Resting *CLEC16A*-deficient

FIGURE 2 CLEC16A co-localizes with Rab4a-positive endosomes in Jurkat T cells. A, B, Quantification of GFP-tagged CLEC16A and Rab4a-, Rab5-mCherry proximity by imaging flow cytometry (IFC). Proximity was calculated using the Bright Detail Similarity feature by the IDEAS software. A, The histograms display the Bright Detail Similarity scores for; left histogram: Hoechst-stained Jurkat T cells transfected with Rab5-mCherry expressing plasmid (negative control) and Jurkat T cells transfected with plasmids expressing Rab4a-GFP and Rab4a-mCherry (positive control), middle histogram: Jurkat T cells co-transfected with plasmids expressing GFP-CLEC16A and Rab4a-mCherry, right histogram: Jurkat T cells co-transfected with plasmids expressing GFP-CLEC16A and Rab5-mCherry. The histograms represents one out of three independent experiments. B, The graph shows the ratio of cells with proximal localization between CLEC16A and TGN46 (n = 1), Rab5 (n = 3), Rab4a (n = 3) or LAMP1 (n = 1) relative to the Rab4a-mCherry/Rab4a-GFP-positive control with SEM. C, Confocal images of Jurkat T cells co-transfected with plasmids encoding GFP-CLEC16A and the indicated Rab-constructs, or GFP-CLEC16A expressing Jurkat T cells, fixed with PFA, permeabilized and stained with antibodies against TGN46 or LAMP1. All cells were stained with Hoechst. Indicated areas are enlarged and arrowheads represent the strong signals at the same location in each image. Scale bar = 10 μm. The images show one representative cell in one out of three experiments. In each experiment, 20-50 cells were analysed. GFP-CLEC16A is illustrated in green, the cellular marker in red and the Hoechst-stained nucleus in blue

Jurkat T cells displayed approximately 15% lower cell surface expression of TCR compared to control cells (Figure 4C, D; $P = .032$). After 40 minutes incubation at 37°C, approximately 50% of the TCRs were internalized (Figure S2C). When allowing for re-emergence of TCR back to the cell membrane, *CLEC16A* suppression resulted in a slightly reduced TCR re-emergence after 10 minutes (Figure 4E). However, this effect disappeared after 20 and 40 minutes of incubation.

3.5 | CLEC16A displays no major effect on T cell activation

C-type lectin-like domain family 16 member A suppression did not have a major effect on TCR recycling, however, we found indications that this may affect the steady-state cell surface levels of TCR (Figure 4C, D). We therefore analysed whether CLEC16A expression affected T cell responses in vitro. *CLEC16A*-deficient Jurkat T cells (Figure 5A, B, left blot) were activated with plate-bound anti-CD3 antibodies (clone OKT3) for 4, 24 and 48 hours prior to analysis of cell surface expression of CD69 (Figure 5C, D). There was a slight, but significant increase in the expression of the T cell activation marker CD69 in the CD69+ cell populations after 4 and 24 hours of activation compared to control cells (Figure 5D, left graph; $P = .048$ and $P = .0028$, respectively), however, this difference did not persist after 48 hours of activation. Although the level of CD69 expression was increased in the CD69+ population after 4 and 24 hours, the percentage of CD69+ cells was slightly, but significantly lower after *CLEC16A* knock-down (24 hours activation) (Figure 5D, right graph; $P = .015$), probably reflecting the reduced steady-state TCR cell surface expression in these cells. In compliance with the data from *CLEC16A*-deficient cells, overexpression of CLEC16A (Figure 5B, right blot) resulted in a small decrease in CD69 expression of the CD69+ population, visible 48 hours after activation (Figure 5E, F, left graph; $P = .0010$). In line with the knock-down experiments, the percentage of CD69+

cells was slightly, but significantly higher after overexpression of CLEC16A and activation for 24 hours (Figure 5F, right graph; $P = .040$). In contrast to the observations in OKT3 stimulated cells, in cells activated with PMA and ionomycin, which directly activates cells via protein kinase C bypassing TCR, CD69 cell surface expression was not affected by CLEC16A knock-down (Figure 5G, H; $P = .11$). These results indicate that CLEC16A overexpression or knock-down gives rise to marginal differences in T cell activation responses through the TCR as measured by cell surface expression of CD69.

To complement the studies in Jurkat T cells, we transfected human, primary CD4+ T cells with *CLEC16A*-specific siRNA or control siRNA (Figure 6A) prior to activation with anti-CD3/CD28-coated beads. Flow cytometry analysis revealed that 24 hours after initiation of activation, all CD4+ T cells expressed high levels of CD69 (Figure 6B, left histogram). In compliance with the data from Jurkat cells, *CLEC16A*-deficient CD4+ T cells expressed marginally higher levels of CD69 ($P = .035$) compared to control cells (Figure 6C, left histogram). However, when analysing later activation markers such as HLA-DR and CD25, *CLEC16A* knock-down did not impact cell surface expression of these markers (Figure 6B, C), suggesting that CLEC16A does not have a major impact on T cell activation.

4 | DISCUSSION

Being associated with a broad spectre of autoimmune disorders, CLEC16A is likely to play a general role in immune-mediated processes (reviewed in[53]). Here, we show that *CLEC16A* expression is induced in CD4+ T cells upon activation, and by the use of Jurkat T cells, we show that it has a T cell-specific sub-localization to Rab4a-positive recycling endosomes and is co-localized with TCR upon internalization. Knock-down and overexpression studies in T cells show no or marginal effects of CLEC16A on starvation-induced cell death or T cell activation response.
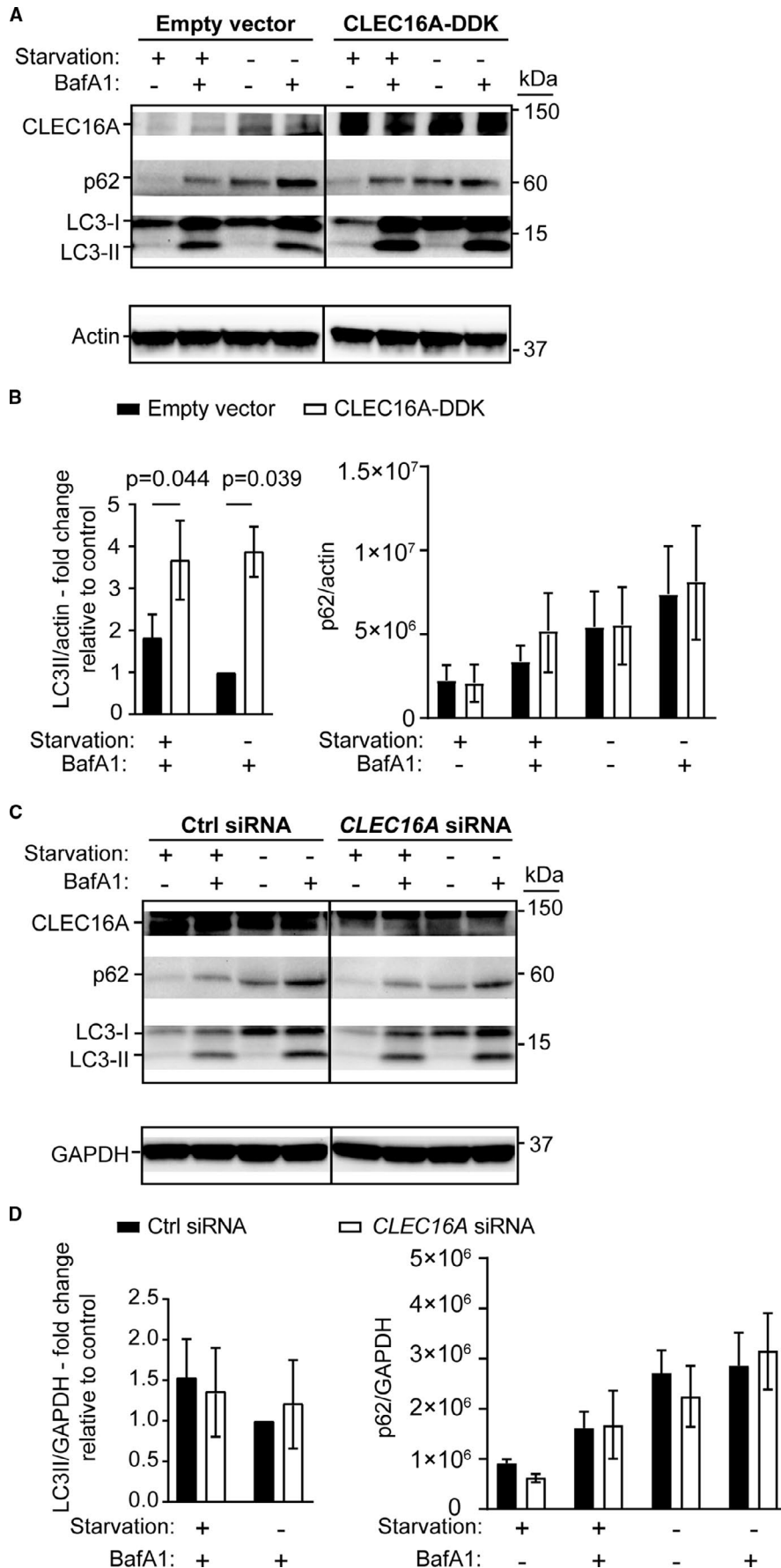
A

B

C

D

FIGURE 3 Overexpression of *CLEC16A* increases autophagic flux in Jurkat T cells. Jurkat T cells transfected with *CLEC16A*-specific siRNA, Ctrl siRNA, vector expressing myc-DKK-tagged CLEC16A or empty vector were kept in normal medium or starved, with or without the presence of BafA1 for 4 h. A, Representative Western blot of lysates from one experiment from cells transfected with myc-DDK-tagged CLEC16A or empty vector, immunoblotted for CLEC16A, p62, LC3 and actin (n = 3). B, The graphs display the quantification of LC3II (left graph) signal relative to actin in the samples with inhibitor BafA1 present (unstarved cells set to 1) and quantification of p62 (right graph) relative to actin in samples with or without the inhibitor present (n = 3). C, Western blot from one representative experiment of lysates from cells transfected with CLEC16A-specific siRNA or Ctrl siRNA, immunoblotted for CLEC16A, p62, LC3 and GAPDH (n = 3). D, The graphs display the quantification of the LC3II (left graph) signal relative to GAPDH in the samples with inhibitor BafA1 present (unstarved cells set to 1) and quantification of p62 (right graph) relative to GAPDH in samples with and without the inhibitor present (n = 3). In (B and D), the mean values with SEM are displayed. The data were analysed with a paired, two-tailed Student's *t* test or a one sample *t* test for normalized data. *P*-values <.05 are considered significant
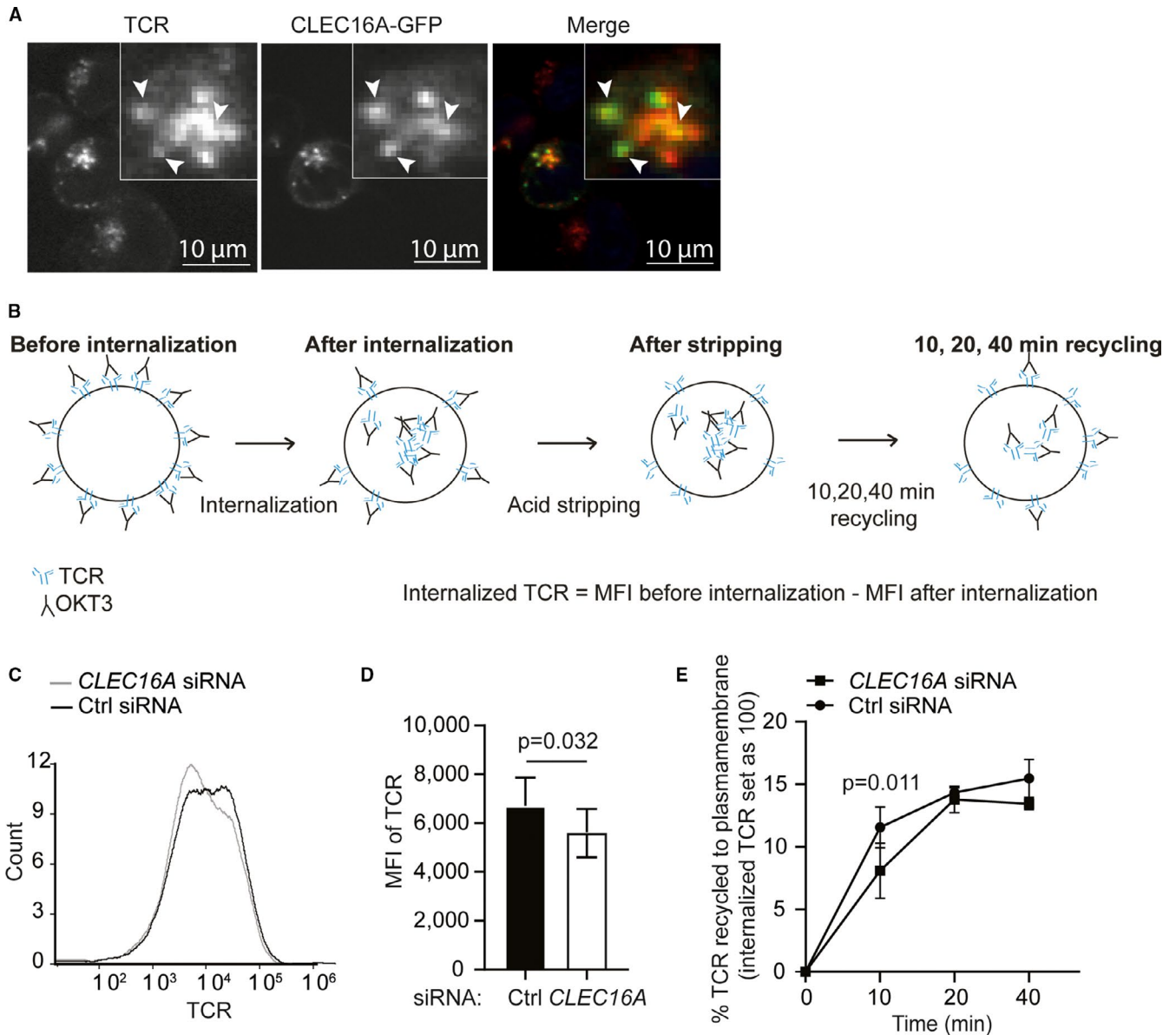
FIGURE 4 *CLEC16A* knock-down results in reduced TCR re-emergence at the cell membrane after stimulation of Jurkat T cells. A, Cells expressing GFP-tagged CLEC16A were labelled with OKT3 (anti-CD3) before receptor internalization and subsequently stained with secondary antibodies against OKT3. Framed areas are enlarged, and arrowheads represent the strong signals at the same location in each image. Scale bar = 10 μm, images from one representative cell from one out of two independent experiments where 30-50 cells/experiment were analysed. B, Schematic drawing showing the procedure used to measure TCR internalization and re-emergence back to the cell membrane. In each step, ('before internalization', 'after internalization', 'after stripping' and 'after recycling') samples were analysed by flow cytometry for cell surface expression of TCR. (C-E) Jurkat T cells co-transfected with *CLEC16A* siRNA (grey) or Ctrl siRNA (black) and EGFP-N3. C, A representative histogram displaying cell surface level of TCR (using APC-conjugated anti-TCR, clone IP26). D, The plot shows the MFI of TCR in the GFP$^+$ cell population (n = 3). E, The cells were surface labelled with OKT3 (anti-CD3). The OKT3-bound complexes were allowed to internalize and the remaining antibodies at the cell surface after internalization were stripped off, and the internal TCR-OKT3 complex were allowed to re-emerge to the surface for the indicated time points. The re-emerged OKT3 antibodies at the cell surface were stained and measured by flow cytometry. The graph displays the mean of the percentage re-emerged TCR from the internal pool (internalized TCR were measured by $MFI_{before\ internalization}$-$MFI_{after\ internalization}$). The data in (D and E) are presented with error bars representing the SEM from >three independent experiments with duplicates. The data were analysed with a paired, two-tailed Student's t test, and P-values <.05 are considered significant. MFI, Median fluorescence intensity

This study was mainly performed using the lymphoblastic Jurkat T cell line, which is frequently used for T cell studies, since the cell line is easy to access, grow and transfect. However, immortalized cells may have additional abnormalities. The Jurkat T cell line lacks the proteins PTEN and SHIP that eventually influence the mTOR pathway causing them to be partly activated in their 'resting' state.[54-56] Therefore, Jurkat cells may show discrepancy compared to
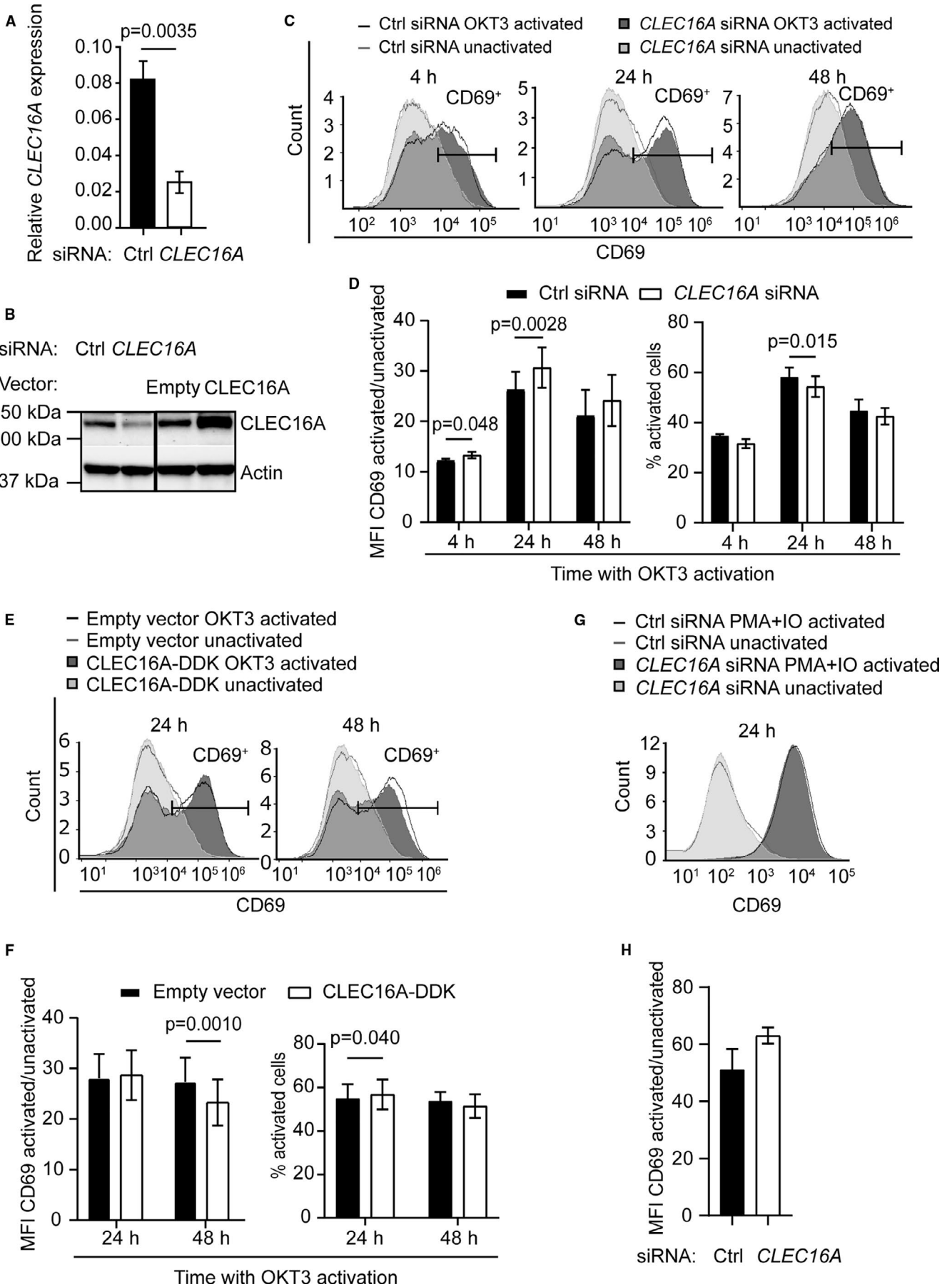
FIGURE 5 CLEC16A affects cell surface expression of CD69 in Jurkat T cells. Jurkat T cells transfected with *CLEC16A* specific siRNA or Ctrl siRNA (A, B, C, D, G and H), or vector expressing myc-DKK-tagged CLEC16A or empty vector (B, E and F) were co-transfected with pEGFP-N3. A, The graph shows mean expression of *CLEC16A* relative to *TBP* measured 48 h after transfection. B, One representative Western blot verifying CLEC16A knock-down (left) and overexpression (right) at protein level. C-F, The cells were activated with OKT3 for indicated time points prior to measurement of CD69 expression of the GFP^{+} cells by flow cytometry. C, The plots show transfected cells (GFP^{+}) from one representative experiment out of at least three. D, The left graph displays the MFI of transfected CD69^{+} cells in activated cells/MFI in inactivated cells (4 h: n = 3, 24 h: n = 7, 48 h: n = 4). The right graph shows the percentage of CD69^{+} cells at indicated time points. E-F, Cell surface expression of CD69 was measured by flow cytometry in GFP^{+} cells (n=4). E, The plots display CD69 expression in GFP^{+} cells from one representative experiment. F, The left graph shows the MFI of transfected CD69^{+} cells in activated cells/MFI in inactivated cells at indicated time points. The right graph shows the percentage of CD69^{+} cells after activation . G and H, SiRNA transfected cells were activated for 24 h with PMA + ionomycin prior to measurement of CD69 expression of the GFP^{+} cells by flow cytometry (n = 4). G, Overlay from one representative experiment. H, The graph displays the MFI of CD69 in the GFP^{+} cells in activated cells/ the MFI of CD69 in inactivated cells. Graphs in (A, D, F and H) represent the mean ± SEM, and the data were analysed with a paired two-tailed Student's *t* test. *P*-values below .05 are considered significant. MFI, Median fluorescence intensity

FIGURE 6 *CLEC16A* knock-down affects cell surface expression of CD69 in CD4^{+} T cells. (A-C) CD4^{+} T cells isolated from healthy donors (n = 3) were co-transfected with control siRNA (Ctrl) or *CLEC16A* siRNA . A, The graph shows mean expression with SEM of *CLEC16A* expression relative to *RNaseP* 24 h after transfection, normalized to control samples (Ctrl). B, The cells were activated for 24 or 48 h with anti-CD3/CD28-coated beads prior to measurement of cell surface expression of CD69 (24 h) or HLA-DR and CD25 (48 h) by flow cytometry. The overlays showdata from one representative experiment. C, The graphs display the mean MFI with SEM of CD69, CD25 and HLA-DR(n = 3). Data are analysed by paired, two-tailed Student's *t* test, *P*-values <.05 are considered significant. MFI, Median fluorescence intensity
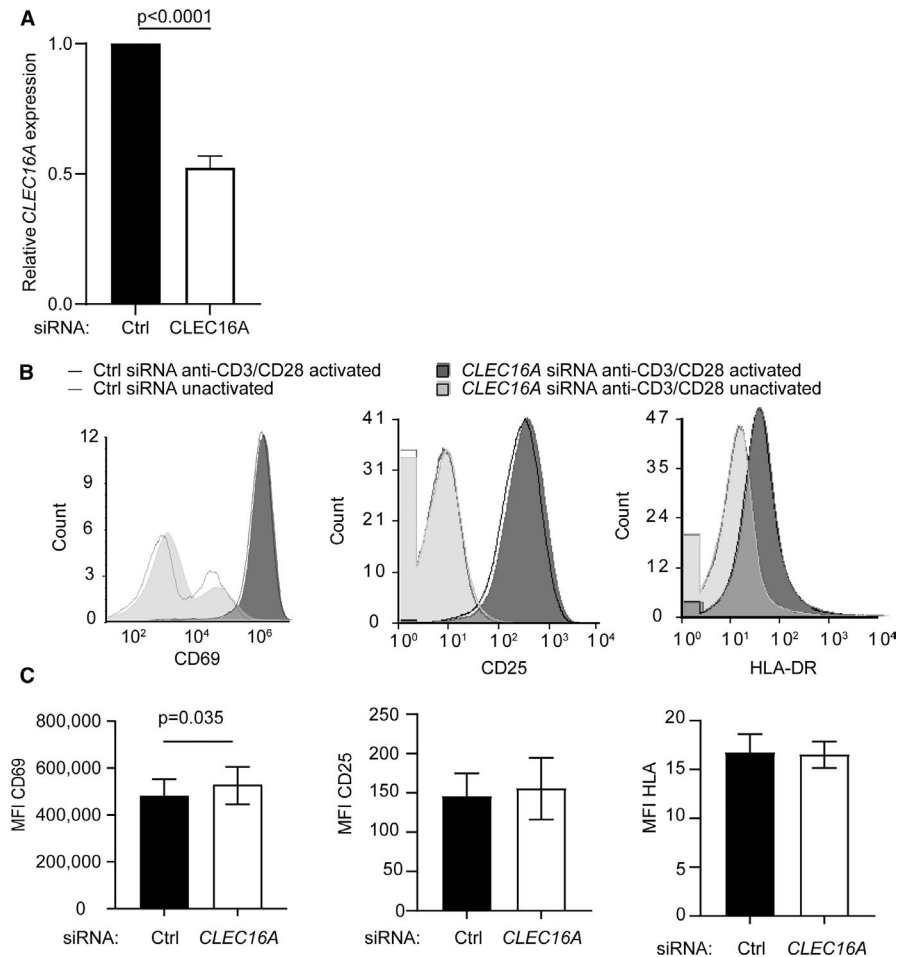
primary T cells and results based solely on experiments with Jurkat cells should therefore be interpreted with caution when translating this to primary T cells.

In the absence of existing CLEC16A antibodies that were suitable for immunofluorescence studies, we overexpressed CLEC16A in fusion with a GFP-tag to monitor its subcellular localization. The position of the tag might affect subcellular localization, as we observed no co-localization to Rab5 in cells transfected with N-terminally GFP-tagged CLEC16A, but partial co-localization in a small fraction of cells when transfecting with C-terminally GFP-tagged CLEC16A.

Internalization and receptor recycling of the TCR are important processes for regulation and duration of TCR signalling in T cells.[50,51] CLEC16A has in other receptor systems been shown to mediate regulation of cell surface receptors, such as the epidermal growth factor receptor at steady state in HeLa cells,[24] the HLA-DR in human

monocyte-derived dendritic cells[30] and various NK cells receptors in murine NK cells,[31] and these data suggest that CLEC16A may be a general regulator of the expression of (a subset) of cell surface molecules. Down-modulation of TCR is a pivotal event during T cell activation. The internalization rate is not increased following TCR ligation, but the TCR down-modulation following T cell activation is suggested to be mediated by intracellular retention of ligated complexes.[50] Indeed, the absence of CLEC16A did influence the rate of rapid TCR recycling back to the cell surface upon TCR ligation, but did not last beyond 10 minutes. It is questionable that such small and transient changes do impact biological processes, and more refined analyses in T cells are necessary to address whether CLEC16A could be involved in fine-tuning of T cell responses either downstream of TCR or other receptors. In other cell systems, CLEC16A has been shown to interact with the CART complex (Hrs/Actinin-4/BERP/Myosin V protein complex)[31] necessary for receptor recycling from Rab5 and back to the plasma membrane.[57] Whether CLEC16A acts via the CART complex in T cells to influence receptor recycling is still to be determined.

Most biological systems display a certain level of redundancy, in the sense that several molecules may fulfil overlapping functions. Our data clearly show that CLEC16A is not essential for TCR activation, and it is questionable whether the observed small alterations in the T cell response will be sufficient to have impact on the immune homeostasis in vivo. Of note, after T cell activation through the TCR, *CLEC16A* knock-down led to fewer activated Jurkat T cells (Figure 5D, right graph), however, this is more likely a result of the reduced TCR cell surface expression prior to activation.

Another recent study has reported that CLEC16A is a regulator of the mTOR pathway,[28] which affects autophagy, T cell activation and differentiation.[58] Activation of mTOR has been shown to drive recycling of T cell surface receptors by Rab4- and Rab5-positive endosomes.[59] In the current work, we showed that CLEC16A co-localizes with Rab4a-positive endosomes during steady state, and with TCRs upon receptor internalization. Whether CLEC16A regulates the cell surface receptors on T cells directly by acting on the internalization and recycling processes or more indirectly by regulating the mTOR pathway in T cells remains to be studied. However, regulation of the mTOR pathway could explain the many diverse functions reported for CLEC16A in different cell types, including autophagy, as the mTOR pathway and autophagy are highly integrated.[46,60]

Several studies show that CLEC16A is emerging as an autophagic regulator[23,24,27,28,31] including in NK cells where CLEC16A overexpression promoted autophagy.[31] This is in line with our own observation of increased autophagic flux in cells with ectopic CLEC16A expression. On the other hand, the effect seen in our CLEC16A overexpression system is not corroborated by our experiments with *CLEC16A*-deficient cells. Therefore, we cannot exclude the possibility that the effect observed in our system is due to artefacts of overexpression. Further work is needed to make firm conclusions on the role of CLEC16A on autophagy in T cells. An intriguing possibility is however that the common denominator for the CLEC16A effect is its association to Rab4a, which both regulates receptor recycling and is known to be a donator of autophagic membranes.[46,48,50,51]

CLEC16A contains a truncated C-type lectin-like domain (CTLD), consisting of only 24 amino acids, whereas a regular CTLD consists of 105 amino acids.[14] Unlike most C-type lectins, CLEC16A is an intracellular protein. Its subcellular localization varies between different cell types, and the localization to Rab4a recycling endosomes has until now not been found in other cells. CLEC16A has been observed in endosomal compartments including late endosomes in monocytic-derived dendritic cells[30] and Drosophila Garland cells,[21] and in lysosomes in Min-6β cells[25] and Drosophila Garland cells[21] in addition to endoplasmic reticulum in K562 cells,[45] the Golgi apparatus in 293T cells,[28] in autophagosomes in Drosophila fat body cells[22] and in the cytosol in the YTS NK cell line.[31] Additional studies are required to define whether co-localization of CLEC16A to Rab4a and partial co-localization to Rab5 is T cell-specific.

While indirect effects of CLEC16A on T cells have previously been reported,[23,45] this is the first study to analyse its localization and function in T cells and the first to find it localized in recycling endosomes. Whereas *CLEC16A* knock-down in lymphoblastic cells did not affect CD4+ T cell activation or proliferation in a co-culturing experiment,[45] CLEC16A affected T cell selection and reactivity in a murine model by regulating autophagy in thymic epithelial cells.[23] Our data show that CLEC16A expression is induced in T cells upon activation, which suggests that it may have a role in those cells. However, further studies are needed in order to delineate whether Rab4a/Rab5 localized CLEC16A has a major function in T cell biology and to unravel whether CLEC16A functions in T cells may contribute to explain its association with a wide variety of autoimmune disorders.

AUTHOR CONTRIBUTIONS

AME performed experiments, collected, analysed and interpreted data, wrote the manuscript and approved the final version of the manuscript. ISL performed experiments, collected, analysed and interpreted data, wrote the manuscript and approved the final version of the manuscript. GA supervised the study, analysed and interpreted data, revised the manuscript and approved the final version of the manuscript. VSG interpreted data and revised the manuscript and approved the final version of the manuscript. MMI performed experiments, collected, analysed and interpreted data, wrote the manuscript and approved the final version of the manuscript. PKK performed experiments, revised the manuscript and approved the final version of the manuscript. TR collected and interpreted data, revised the manuscript and approved the final version of the manuscript. OJBL supervised the study, analysed and interpreted data, revised the manuscript and approved the final version of the manuscript. SDB analysed and interpreted data, revised the manuscript and approved the final version of the manuscript. HFH conceived and designed the study, revised the manuscript and approved the final version of the manuscript. AS conceived and designed the study, interpreted the data, wrote the manuscript and approved the final version of the manuscript. TB conceived and designed the study, performed experiments, acquired, analysed and interpreted data, wrote the manuscript and approved the final version of the manuscript.

ETHICAL APPROVAL

The Regional Committee for Medical and Health Research Ethics South East, Norway, approved the study and the experimental protocols used. The experiments were performed in accordance with the approval, and written informed consent was obtained from study participants.

DATA AVAILABILITY STATEMENT

The data that support the findings of this study are available from the corresponding author upon reasonable request.

ORCID

Torbjørn Rognes https://orcid.org/0000-0002-9329-9974
Anne Spurkland https://orcid.org/0000-0003-4421-0766
Tone Berge https://orcid.org/0000-0002-5297-2034

REFERENCES

1. International Multiple Sclerosis Genetics C, Hafler DA, Compston A, et al. Risk alleles for multiple sclerosis identified by a genome-wide study. *N Engl J Med*. 2007;357:851-862.
2. Australia, New Zealand Multiple Sclerosis Genetics C. Genome-wide association study identifies new multiple sclerosis susceptibility loci on chromosomes 12 and 20. *Nat Genet*. 2009;41:824-828.
3. Hoppenbrouwers IA, Aulchenko YS, Janssens AC, et al. Replication of CD58 and CLEC16A as genome-wide significant risk genes for multiple sclerosis. *J Hum Genet*. 2009;54:676-680.
4. Sawcer S, Hellenthal G, Pirinen M, et al. Genetic risk and a primary role for cell-mediated immune mechanisms in multiple sclerosis. *Nature*. 2011;11(476):214-219.
5. Zoledziewska M, Costa G, Pitzalis M, et al. Variation within the CLEC16A gene shows consistent disease association with both multiple sclerosis and type 1 diabetes in Sardinia. *Genes Immun*. 2009;10:15-17.
6. Johnson BA, Wang J, Taylor EM, et al. Multiple sclerosis susceptibility alleles in African Americans. *Genes Immun*. 2010;11:343-350.
7. Nischwitz S, Cepok S, Kroner A, et al. More CLEC16A gene variants associated with multiple sclerosis. *Acta Neurol Scand*. 2011;123:400-406.
8. Mero I-L, Ban M, Lorentzen ÅR, et al. Exploring the CLEC16A gene reveals a MS-associated variant with correlation to the relative expression of CLEC16A isoforms in thymus. *Genes Immun*. 2011;12:191-198.
9. Zuvich RL, Bush WS, McCauley JL, et al. Interrogating the complex role of chromosome 16p13.13 in multiple sclerosis susceptibility: independent genetic signals in the CIITA-CLEC16A-SOCS1 gene complex. *Hum Mol Genet*. 2011;1(20):3517-3524.
10. Patsopoulos NA, Baranzini SE, Santaniello A, et al. Multiple sclerosis genomic map implicates peripheral immune cells and microglia in susceptibility. *Science*. 2019;365(6460):eaav7188.
11. Beecham AH, Patsopoulos NA, Xifara DK, et al. Analysis of immune-related loci identifies 48 new susceptibility variants for multiple sclerosis. *Nat Genet*. 2013;45:1353-1360.
12. Hakonarson H, Grant SFA, Bradfield JP, et al. A genome-wide association study identifies KIAA0350 as a type 1 diabetes gene. *Nature*. 2007;2(448):591-594.
13. Consortium WTCC. Genome-wide association study of 14,000 cases of seven common diseases and 3,000 shared controls. *Nature*. 2007;7(447):661-678.
14. Todd JA, Walker NM, Cooper JD, et al. Robust associations of four new chromosome regions from genome-wide analyses of type 1 diabetes. *Nat Genet*. 2007;39:857-864.
15. Cooper JD, Smyth DJ, Smiles AM, et al. Meta-analysis of genome-wide association study data identifies additional type 1 diabetes risk loci. *Nat Genet*. 2008;40:1399-1401.
16. Barrett JC, Clayton DG, Concannon P, et al. Genome-wide association study and meta-analysis find that over 40 loci affect risk of type 1 diabetes. *Nat Genet*. 2009;41:703-707.
17. Márquez A, Varadé J, Robledo G, et al. Specific association of a CLEC16A/KIAA0350 polymorphism with NOD2/CARD15(-) Crohn's disease patients. *Eur J Hum Genet*. 2009;17:1304-1308.
18. Skinningsrud B, Husebye ES, Pearce SH, et al. Polymorphisms in CLEC16A and CIITA at 16p13 are associated with primary adrenal insufficiency. *J Clin Endocrinol Metab*. 2008;93:3310-3317.

19. Martínez A, Perdigones N, Cénit MC, et al. Chromosomal region 16p13: further evidence of increased predisposition to immune diseases. *Ann Rheum Dis*. 2010;69:309-311.

20. Skinningsrud B, Lie BA, Husebye ES, et al. A CLEC16A variant confers risk for juvenile idiopathic arthritis and anti-cyclic citrullinated peptide antibody negative rheumatoid arthritis. *Ann Rheum Dis*. 2010;69:1471-1474.

21. Kim S, Wairkar YP, Daniels RW, DiAntonio A. The novel endosomal membrane protein Ema interacts with the class C Vps-HOPS complex to promote endosomal maturation. *J Cell Biol*. 2010;8(188):717-734.

22. Kim S, Naylor SA, DiAntonio A. Drosophila golgi membrane protein Ema promotes autophagosomal growth and function. *Proc Natl Acad Sci USA*. 2012;1(109):E1072-E1081.

23. Schuster C, Gerold K, Schober K, et al. The autoimmunity-associated gene CLEC16A modulates thymic epithelial cell autophagy and alters T cell selection. *Immunity*. 2015;19(42):942-952.

24. Redmann V, Lamb CA, Hwang S, et al. Clec16a is critical for autolysosome function and purkinje cell survival. *Sci Rep*. 2016;18(6):23326.

25. Soleimanpour S, Gupta A, Bakay M, et al. The diabetes susceptibility gene Clec16a regulates mitophagy. *Cell*. 2014;19(157): 1577-1590.

26. Pearson G, Chai B, Vozheiko T, et al. Clec16a, Nrdp1, and USP8 form a ubiquitin-dependent tripartite complex that regulates beta-cell mitophagy. *Diabetes*. 2018;67:265-277.

27. Pandey R, Bakay M, Strenkowski BP, Hain HS, Hakonarson H. JAK/STAT inhibitor therapy partially rescues the lipodystrophic autoimmune phenotype in Clec16a KO mice. *Sci Rep*. 2021;1(11):7372.

28. Tam RCY, Li MWM, Gao YP, et al. Human CLEC16A regulates autophagy through modulating mTOR activity. *Exp Cell Res*. 2017;15(352):304-312.

29. Pandey R, Bakay M, Hain HS, et al. CLEC16A regulates splenocyte and NK cell function in part through MEK signaling. *PLoS One*. 2018;13:e0203952.

30. van Luijn MM, Kreft KL, Jongsma ML, et al. Multiple sclerosis-associated CLEC16A controls HLA class II expression via late endosome biogenesis. *Brain*. 2015;138:1531-1547.

31. Pandey R, Bakay M, Hain HS, et al. The autoimmune disorder susceptibility gene CLEC16A restrains NK cell function in YTS NK cell line and Clec16a knockout mice. *Front Immunol*. 2019;10:68.

32. Farh K-H, Marson A, Zhu J, et al. Genetic and epigenetic fine mapping of causal autoimmune disease variants. *Nature*. 2015;19(518):337-343.

33. Maurano MT, Humbert R, Rynes E, et al. Systematic localization of common disease-associated variation in regulatory DNA. *Science*. 2012;7(337):1190-1195.

34. Leikfoss IS, Keshari PK, Gustavsen MW, et al. Multiple sclerosis risk allele in CLEC16A acts as an expression quantitative trait locus for CLEC16A and SOCS1 in CD4+ T cells. *PLoS One*. 2015;10:e0132957.

35. Skjeldal FM, Strunze S, Bergeland T, Walseng E, Gregers TF, Bakke O. The fusion of early endosomes induces molecular-motor-driven tubule formation and fission. *J Cell Sci*. 2012;15(125):1910-1919.

36. Naderi S, Blomhoff HK. Retinoic acid prevents phosphorylation of pRB in normal human B lymphocytes: regulation of cyclin E, cyclin A, and p21(Cip1). *Blood*. 1999;15(94):1348-1358.

37. Pandya AD, Al-Jaderi Z, Høglund RA, et al. Identification of human NK17/NK1 cells. *PLoS One*. 2011;6:e26780.

38. Kolseth IB, Agren J, Sundvold-Gjerstad V, Lyngstadaas SP, Wang JE, Dahle MK. 9-cis retinoic acid inhibits inflammatory responses of adherent monocytes and increases their ability to induce classical monocyte migration. *J Innate Immun*. 2012;4:176-186.

39. Bos SD, Page CM, Andreassen BK, et al. Genome-wide DNA methylation profiles indicate CD8+ T cell hypermethylation in multiple sclerosis. *PLoS One*. 2015;10(3):e0117403.

40. Clipstone NA, Crabtree GR. Identification of calcineurin as a key signalling enzyme in T-lymphocyte activation. *Nature*. 1992;25(357):695-697.

41. Granum S, Sundvold-Gjerstad V, Gopalakrishnan RP, et al. The kinase Itk and the adaptor TSAd change the specificity of the kinase Lck in T cells by promoting the phosphorylation of Tyr192. *Sci Signal*. 2014;7(355):ra118.

42. Zuba-Surma EK, Kucia M, Abdel-Latif A, Lillard JW Jr, Ratajczak MZ. The imagestream system: a key step to a new era in imaging. *Folia Histochem Cytobiol*. 2007;45:279-290.

43. BioGPS Gene Annotation Portal. BioGPS; A free extensible and customizable gene annotation portal, a complete resource for learning about gene and protein function. www.biogps.org. Accessed May 12, 2021.

44. National Institutes of Health. The genotype-tissue expression portal. 2019; https://www.gtexportal.org/home/. Accessed May 12, 2021.

45. Zouk H, D'Hennezel E, Du X, Ounissi-Benkalha H, Piccirillo CA, Polychronakos C. Functional evaluation of the role of C-type lectin domain family 16A at the chromosome 16p13 locus. *Clin Exp Immunol*. 2014;175:485-497.

46. Talaber G, Miklossy G, Oaks Z, et al. HRES-1/Rab4 promotes the formation of LC3(+) autophagosomes and the accumulation of mitochondria during autophagy. *PLoS One*. 2014;9:e84392.

47. Puri C, Renna M, Bento CF, Moreau K, Rubinsztein DC. Diverse autophagosome membrane sources coalesce in recycling endosomes. *Cell*. 2013;12(154):1285-1299.

48. Tanida I, Ueno T, Kominami E. LC3 and autophagy. *Methods Mol Biol*. 2008;445:77-88.

49. Bjørkøy G, Lamark T, Pankiv S, Øvervatn A, Brech A, Johansen T. Monitoring autophagic degradation of p62/SQSTM1. *Methods Enzymol*. 2009;452:181-197.

50. Liu H, Rhodes M, Wiest DL, Vignali DA. On the dynamics of TCR:CD3 complex cell surface expression and downmodulation. *Immunity*. 2000;13:665-675.

51. Das V, Nal B, Dujeancourt A, et al. Activation-induced polarized recycling targets T cell antigen receptors to the immunological synapse; involvement of SNARE complexes. *Immunity*. 2004;20:577-588.

52. Patrussi L, Baldari CT. Analysis of TCR/CD3 recycling at the immune synapse. *Methods Mol Biol*. 2017;1584:143-155.

53. Berge T, Leikfoss IS, Harbo HF. From identification to characterization of the multiple sclerosis susceptibility gene CLEC16A. *Int J Mol Sci*. 2013;14:4476-4497.

54. Shan X, Czar MJ, Bunnell SC, et al. Deficiency of PTEN in Jurkat T cells causes constitutive localization of Itk to the plasma membrane and hyperresponsiveness to CD3 stimulation. *Mol Cell Biol*. 2000;20:6945-6957.

55. Wang X, Gjorloff-Wingren A, Saxena M, Pathan N, Reed JC, Mustelin T. The tumor suppressor pten regulates T cell survival

and antigen receptor signaling by acting as a phosphatidylinositol 3-phosphatase. *J Immunol*. 2000;164(4):1934-1939.

56. Seminario MC, Wange RL. Signaling pathways of D3-phosphoinositide-binding kinases in T cells and their regulation by PTEN. *Semin Immunol*. 2002;14:27-36.

57. Yan Q, Sun W, Kujala P, Lotfi Y, Vida TA, Bean AJ. CART: an Hrs/actinin-4/BERP/myosin V protein complex required for efficient receptor recycling. *Mol Biol Cell*. 2005;16:2470-2482.

58. El Hiani Y, Egom EE, Dong XP. mTOR signalling: jack-of-all-trades (1). *Biochem Cell Biol*. 2019;97:58-67.

59. Fernandez DR, Telarico T, Bonilla E, et al. Activation of mammalian target of rapamycin controls the loss of TCRzeta in lupus T cells through HRES-1/Rab4-regulated lysosomal degradation. *J Immunol*. 2009;182:2063-2073.

60. Dunlop EA, Tee AR. mTOR and autophagy: a dynamic relationship governed by nutrients and energy. *Semin Cell Dev Biol*. 2014;36:121-129.

SUPPORTING INFORMATION

Additional supporting information may be found online in the Supporting Information section.

How to cite this article: Eriksson AM, Leikfoss IS, Abrahamsen G, et al. Exploring the role of the multiple sclerosis susceptibility gene *CLEC16A* in T cells. *Scand J Immunol*. 2021;00:e13050. https://doi.org/10.1111/sji.13050